Neutron-inelastic-scattering measurements on uranium antimonide

G. H. Lander
*Centre d'Etudes Nucleaires, 38041 Grenoble, France and Argonne National Laboratory, Argonne, Illinois 60439**

W. G. Stirling
Institut Laue Langevin, 38042 Grenoble, France

(Received 4 June 1979)

We report neutron-inelastic-scattering measurements on the fcc compound USb, which orders antiferromagnetically at 240 K with the simple type I structure. The phonon spectra in the [ξξ0] and [00ξ] directions are similar to those measured previously in uranium rocksalt systems. The magnetic response consists of three parts: (i) A collective excitation which is longitudinal in nature; i.e., the fluctuations correspond to variations in magnitude of the moment along the quantization axis rather than deviations from this direction. At the magnetic zone center [110] the anisotropy gap is 1.53 ± 0.05 THz and is degenerate with the acoustic-phonon energy at this point. With increasing temperature the excitation rapidly decreases in intensity and cannot be observed for $T > T_N/2$. (ii) A broad, almost temperature-independent excitation centered at ~ 6 THz, which is probably a crystal-field excitation. (iii) A magnetic-response function centered at $E = 0$ but with a half-width that apparently increases with increasing temperature. We are unable to understand these results in a quantitative manner. However, the implications for our understanding of actinide systems, in particular the shortcomings of present models, are discussed.

I. INTRODUCTION

When the first detailed experiments on actinide systems were undertaken more than a decade ago, the general expectation was that the $5f$ and $4f$ series would show many of the same properties. This expectation derived principally from a wealth of spectroscopic information already published on actinide ions in small concentrations in solution. Although the analysis of actinide spectra is complicated by the presence of roughly comparable Coulomb, spin-orbit, and crystal-field interactions, computational methods for unraveling the spectra are available.[1] The considerable success of crystal-field theory in describing the interactions in lanthanide ($4f$) systems, coupled with the similarities between $4f$ and $5f$ ionic spectra, led naturally to the application of lanthanide-type theories to the metallic actinide systems.

The first attempt to collate and explain the many physical measurements performed on UX compounds (X=group Va: N, P, As, Sb, Bi; and X =group VIa: S, Se, Te) came in 1968 by Grunzweig-Genossar *et al.*[2] These compounds are all cubic with rock salt structure, and all order magnetically. Based on a number of arguments, the authors[2] proposed a model in which the uranium atoms are tetravalent ($5f^2$) and the crystal-field ground state is a nonmagnetic singlet. The ordering then develops because of a large exchange mechanism, probably of the Ruderman-Kittel-Kasuya-Yosida (RKKY) type. Following this paper, Chan and Lam[3] did a more complete treatment of the case in which the crystal-field interaction is large and showed the necessity for including spin-orbit coupling and J mixing. For the same UX compounds, they proposed $5f^3$ for U-Va series and $5f^4$ for U-VIa series.

An important consequence of the "crystal-field approach" is that the energy levels of the $5f$ electrons are quantized into discrete crystal-field states. Provided the crystal-field levels are not strongly broadened by exchange or other interactions, they can be identified with neutron spectroscopy, as has been the case in many lanthanide systems.[4] The first neutron experiments on the UX compounds were performed[5] by Wedgwood and Wedgwood and de Novion in 1974. Surprisingly, they showed no sign of any discrete magnetic excitations, although it was clear that magnetic scattering was present. The magnetic scattering is spread over a wide energy range and resembles a Gaussian function as predicted by de Gennes for a localized paramagnet with exchange interaction. These measurements were performed on UN, UP, USe, US, and UTe. Since that time searches with neutron-inelastic scattering have been unsuccessful in attempting to identify discrete levels in most actinide systems.[6] Furrer and Murasik[7] have published some evidence for magnetic scattering in UAs but their identification of the crystal-field scheme from one barely resolved signal seems very ambitious.

The negative results obtained by neutron experiments show that the simple "crystal-field model" is unlikely to be successful in understanding the UX compounds. Of course, such a conclusion had already been argued by Davis[8] from considera-

tions of band theory and the large values of the electronic specific heats observed for many of these materials. Further evidence for the strong interaction of the $5f$ and $6d$ electrons was provided by the photoemission experiments of Eastman and Kuznietz.[9]

Over the last few years three important developments relating to actinide research have taken place. First, experiments on plutonium, americium, and curium systems have shown that for these materials the lanthanide-type model is probably applicable. For example, in PuP, neutron diffraction[10] shows the $5f^5$ nature of the configuration and is able to put a limit on the magnitude of V_4, the fourth-order crystal-field potential. In most americium compounds no magnetic ordering is found,[11] indicating a $J=0$ or $5f^6$ ground state, whereas in curium metal antiferromagnetism is found with $\sim 7\mu_B$ per Cm atom.[12] Although we would like to see more work on the heavier actinide systems, these trends focus interest on the U and Np systems in which the $5f$ electron wave function is most extended. Second, the studies of "intermediate valence" have heralded a new definition of unstable rare-earth ions, most notably cerium, but also Sm, Tm, and Yb. The important point is that although these ions are orbitally degenerate, one does not start from the conventional crystal-field model. Indeed, the crystal-field interaction appears quite small, and neutron-inelastic-scattering[13,14] experiments show a broad Lorentzian distribution of magnetic scattering centered around $E=0$. The half-width of this distribution has been related to the characteristic frequency of the valence fluctuation,[15] although this interpretation may be too simple.[16] Robinson[17] and Robinson and Erdos[18] have argued that uranium compounds must be treated within the framework of intermediate valence, and we hope to present evidence to support their suggestions. Third and by no means least, large crystals of the UX compounds are now being grown by Vogt of the Laboratorium fur Festkorperphysik, Eidgenossische Technische Hochschule, Zurich. This development has allowed us to search for magnetic excitations in $\vec{Q}, \omega$ space with a triple-axis spectrometer and single crystals, rather than using polycrystalline samples, in which only $|\vec{Q}|$ can be selected. A brief report of this work has been published.[19]

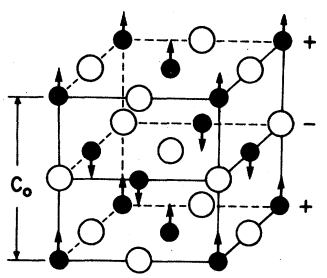

FIG. 1. Uranium antimonide crystal (NaCl) and magnetic (type I) structures. The solid circles are U atoms, the open circles Sb.

In Sec. II, we describe the experimental procedure and the measurements of the phonon spectra. In Sec. III the magnetic scattering, its temperature dependence, and the search for magnon-phonon interactions are presented. Section IV provides a discussion, and a short summary is given in Sec. V.

II. EXPERIMENTAL

A. Previous work

Uranium antimonide (NaCl crystal structure) appears to exist over a range of composition, as indicated by both the lattice parameters (6.176–6.209 Å) and Néel temperatures (217–246 K). The magnetic structure[20] is type I, which consists of ferromagnetic (001) sheets arranged in the simple $+-$ sequence. The spin direction is perpendicular to the sheets, i.e., $\vec{\mu} \parallel [001]$. The crystal and magnetic structures are shown in Fig. 1. This is the same magnetic structure as the lanthanide analog[21] NdSb. A detailed neutron-diffraction study[20] has shown that the moment is $2.8\mu_B$ per U atom and that the magnetization density is oblate in shape at low temperature. An analysis of these results suggested a $5f^3$ configuration with a $\Gamma_8^{(1)}$ quartet as the crystal-field ground state.

The (110) projection of the Brillouin zones of both the nuclear and magnetic structures are shown in Fig. 2. The magnetic structure is C-face centered so that $h+k=$ even and $h+l=$ odd correspond to magnetic Bragg reflections. As shown in Fig. 2 both the magnetic and nuclear reciprocal-lattice points are magnetic zone centers. However, at the nuclear zone centers, normal acoustic spin waves are out of phase, so that we would expect the intensity of these modes to be very small in these zones.[22] This argument will not apply to dispersionless crystal-field levels (excitons), as was shown in Ref. 21.

B. Magnetic domains

So far we neglected the domains present in the magnetic phase. Since the magnetic propagation direction of the magnetic structure $\vec{\tau}$ can be parallel to any of the three cubic axes, three types of domains exist. For *elastic* scattering only one domain contributes at a specific reciprocal-lattice point. For inelastic scattering we must know the dynamical structure factor before being able to assign an experimental neutron group to a certain do-

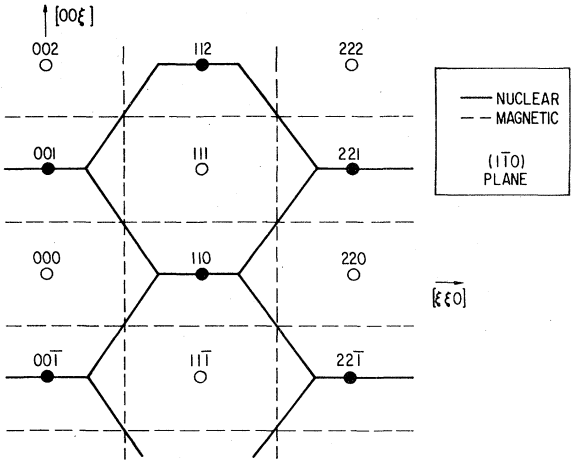

FIG. 2. Nuclear (solid lines) and magnetic (broken lines) Brillouin zones in the (1$\bar{1}$0) plane. For the magnetic case only that zone arising from the c domains, i.e., with $\vec{\mu} \parallel [001]$, is shown.

main. Unfortunately our present lack of understanding of these systems does not permit a detailed calculation of the dynamical structure factor. On the other hand, we can use symmetry relationships to simplify the domain ambiguities. They have been discussed fully by Furrer *et al.*[21] in their examination of the magnetic excitations in NdSb. Let us consider the scattering at the [001] position that arises from the two domains with spins along (100) and (010). Since the spins in these domains are perpendicular to [001], the scattering will arise from both longitudinal and transverse components (see Sec. III A below for a more detailed discussion of this point). In particular, we should expect to see scattering from longitudinal components from the (110) and (010) domains at [001]. However, the [001] is a zone boundary for both the (100) and (010) domains, and we normally expect the dynamical structure factor to decrease as one goes away from the zone center and to be at a minimum at the zone boundary. As we shall see, nothing is seen at or near [0, 0, 1]. This means that there are no transverse excitations for the (001) domains and that the contributions from the other two domains are minimized because of their dynamical structure factor. By using Table II of Ref. 21, we can easily relate the points in high-symmetry directions from different domains, and, provided that measurements are confined to points near the magnetic zone center, that part of the magnetic-response function exhibiting dispersion can be measured from a single domain. In the case of an exciton, or dispersionless crystal-field level, the above arguments about the variation of the dynamical structure factor may be incorrect,[21] and we should expect to see scattering in all parts of the Brillouin zone. We do, in fact, find a mode with such a $\vec{q}$-independent structure factor.

C. Experimental procedure

The experiments have all been performed on a crystal assembly consisting of six oriented single crystals with a total volume of 200 mm^3. The resulting mosaic of the sample was about 1.5°. For magnetic scattering the domains reduce the effective volume by a factor of three. The triple-axis spectrometer IN8 at the Institut Laue Langevin has been used for most measurements, with a few low-energy scans being performed on IN3. For most measurements, a focusing pyrolitic graphite monochromator and flat analyzer were used, PG(002) → PG(002), although for studies at high energy transfers, a copper, Cu(111), monochromator was used. The most intense magnetic scattering observed in our experiments corresponds to ~15 cts/min above a similar inelastic background signal from the sample (the intrinsic background was no greater than 2–3 cts/min), and with such a weak signal we have been forced throughout the experiment to have rather poor collimation, usually 60 min of arc.

The excitation energy $\hbar\omega$ and the momentum transfer $\vec{Q}$ are given by

$$\hbar\omega \equiv \Delta E \equiv \frac{\hbar^2}{2m_n}(k_i^2 - k_f^2) \tag{1}$$

and

$$\vec{Q} = \vec{k}_i - \vec{k}_f , \tag{2}$$

respectively, where k_i is the initial and k_f the final wave vector. ($k = 2\pi/\lambda$ relates the neutron wave vector and wavelength.)

All scans were performed in the constant k_f mode. For low-energy scans $k_f = 2.662$ Å^{-1} was used, which allows a pyrolitic graphite filter to eliminate any possible second-order contamination. However, since the magnetic scattering is proportional to the square of the magnetic form factor $f^2(\vec{Q})$ [our previous study[20] of USb has shown that to a very good approximation $f^2(Q) = \exp(-0.07Q^2)$ for $Q \leq 5$ Å^{-1}] experiments must be confined to small Q, and hence small scattering angles ϕ. In practice, for the spectrometer configuration Cu(111) → PG(002) the maximum energy transfer allowed by geometric considerations was about 10 THz.

D. Phonon measurements

The structure factor for observing one-phonon

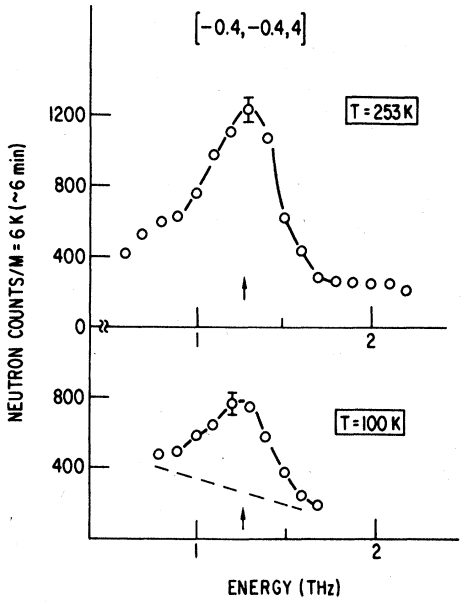

FIG. 3. Transverse acoustic phonons at 253 and 100 K. Measurements taken with PG(002)→PG(002) and $k_f = 3.6$ Å^{-1}.

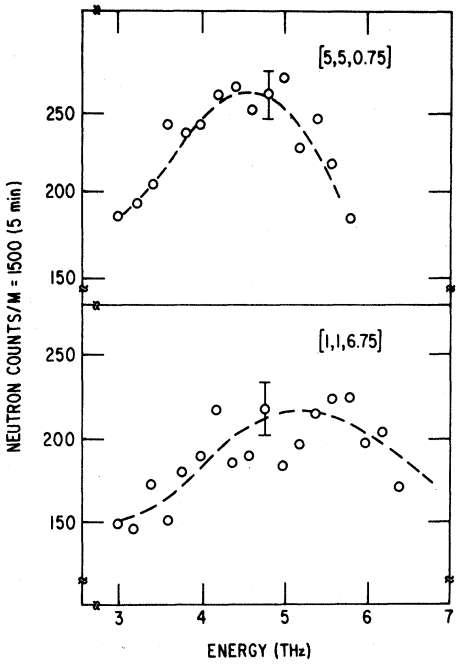

FIG. 4. Optic phonons measured at room temperature. Upper figure shows a transverse optic phonon and lower figure shows a longitudinal optic phonon.

coherent scattering is proportional to $|\vec{Q}|^2$, so that, to discriminate between magnetic and nuclear inelastic scattering, different Q regions are often used. However, the very small magnetic signal in the present investigations means that for intermediate values of the momentum transfer and temperature, the nuclear and magnetic scattering are comparable in intensity.

In Fig. 3 we show scattering from a transverse acoustic phonon measured at 253 and 100 K. As predicted from the Bose population factor, the intensity changes by a factor of 2 on cooling. In the UX compounds with X=N, C the position and dispersion of the optic modes are of interest because the light atoms can be thought of as Einstein oscillators.[5,23,24] This situation does not hold true for USb in which the mass ratio of Sb/U is much greater than N/U so the optic modes should be at a lower frequency and exhibit dispersion. The dispersion of the acoustic-phonon branches is very similar to that found[25] in RbCl, as one might expect from the similar atomic-mass ratios. The optic phonons proved difficult to measure in USb, and full advantage had to be taken of structure-factor effects.[26] Representative optic-phonon groups are shown in Fig. 4. The instrumental resolution function for this configuration is ~1.4 THz. The average optical frequency is close to the value of 4.6 THz determined by Wedgwood and de Novion[5] with time-of-flight experiments.

The phonon dispersion curves in two principal directions are shown together with the magnetic excitations in Fig. 8. Since measurements have not been made in the (001) plane, we have no values for the T_2A mode. The temperature dependence of the phonon frequencies was found to be very small.

III. MAGNETIC SCATTERING

A. Separation of transverse and longitudinal components

The cross section for scattering of neutrons by a magnetic system may be written

$$\frac{d^2\sigma}{d\Omega d\omega} = \left(\frac{\gamma e^2}{2mc^2}\right)^2 \frac{k_f}{k_i} |f(\vec{Q})|^2 \sum_{mn} p_n \left(\left\langle n \left| \sum_l g\vec{J}_\perp \exp(-i\vec{Q}\cdot\vec{r}_l) \right| m \right\rangle\right) \left(\left\langle m \left| \sum_l g\vec{J}_\perp \exp(i\vec{Q}\cdot\vec{r}_l) \right| n \right\rangle\right) \delta\left(\frac{(E_n - E_m)}{\hbar} - \omega\right), \quad (3)$$

where γ is the neutron magnetic moment in nuclear magnetons ($\gamma = 1.91$), $f(\vec{Q})$ is the atomic form factor, and $\vec{J}_\perp$ is the component of the total angular momentum $\vec{J}$ perpendicular to the momentum transfer $\vec{Q}$. The initial state of the crystal is labeled n, has a probability p_n, an energy E_n, and the final state is denoted by m. The operator $\vec{J}_\perp$ can be written in terms of effective spin operators, and the sum is over all atoms in the unit cell. At a later stage we shall calculate a series of matrix elements for one particular model for USb. At this stage, however, it is important to focus attention on the well-known fact that the magnetic interaction selects components perpendicular to $\vec{Q}$, i.e., $\vec{J}_\perp$. Furthermore, the single-domain nature of the scattering (see IIB above) allows us to separate out the transverse and longitudinal components. This possible separation has been exploited previously, most notably by Schulhof *et al.*[27] in the case of MnF_2.

To describe this clearly, we consider the magnetic moment projected into three orthogonal directions [001], [110]. and [$\bar{1}$10], with components J_z, $J_{x'}$, and $J_{y'}$, respectively. The equilibrium direction of the moment is [001]. From Eq. (3) the scattering cross section depends on the operator $\vec{J}_\perp$, which selects components perpendicular to the momentum transfer $\vec{Q}$. If $\vec{Q} \parallel [001]$, the components of interest are therefore $J_{x'}$ and $J_{y'}$. In the sense that these are perpendicular to the equilibrium direction of the moment $\vec{J}$, we call them *transverse* components. We can think of these components as arising from matrix elements $\langle n|J_\pm|m\rangle$ in the usual notation, and they give rise to conventional spin waves. For elastic scattering, since the equilibrium values of $J_{x'}$ and $J_{y'}$ are zero, the cross section itself is zero. No elastic scattering appears at (001); but, if we consider the dynamics of the system, then a precession of the moments around [001] gives rise to $J_{x'}$ and $J_{y'}$ components, and thus neutron-inelastic scattering should be observed. A direct confirmation of these arguments may be found in Ref. 27, and in the study[28] on TbSb. In TbSb the spins are along $\langle 111\rangle$, so no elastic scattering occurs at $(\frac{1}{2}\frac{1}{2}\frac{1}{2})$, but a well-defined spin wave is observed there (see Fig. 3 of Ref. 28).

Now let us place $\vec{Q} \parallel [110]$. The components perpendicular to the momentum transfer, and therefore contributing to the cross section, are J_z and $J_{y'}$. The J_z component we call *longitudinal*, and it corresponds to fluctuations in the magnitude of $|\vec{J}|$. In the case of $\vec{Q} \parallel [110]$ we see both transverse $J_{y'}$ and longitudinal J_z components, the so-called "mixed" scattering discussed in Ref. 27. Hence by looking at scattering near both [001] and [110] we can, in principle, determine the longitudinal (J_z matrix elements) and transverse ($J_\pm$ matrix elements) parts of the spectrum separately.

B. Results at low temperature

The results of constant-$\vec{Q}$ scans at [110] and at and near the [001] point are shown in Figs. 5(a) and 5(b). Recalling the previous section, we can immediately tell from the absence of scattering at [001] that the mode at [110] is predominantly *longitudinal* in character. We have observed the mode at [110] with a number of spectrometer configurations and in each case found no sign of a well-defined neutron group at the same energy at [001]. In Fig. 5(c) is presented the result of a constant-energy scan at an energy just below that of the mode at [110], and no peak is observable. The mode at 1.5 THz is therefore the lowest-energy collective magnetic mode of the system.

Since [110] is the magnetic zone center, we would expect the magnetic excitations to have their lowest energy at this point. This is indeed the case. In Figs. 6 and 7 we show scans at different reduced-q values across the zone. As $|q|$ is increased we appear to observe a second mode, with an energy of between 5 and 7 THz. The collective excitation apparently disappears into this mode, and kinematic restrictions prevent further observations at higher energy transfers. Particular note should be made of the lower two scans in Fig. 7.

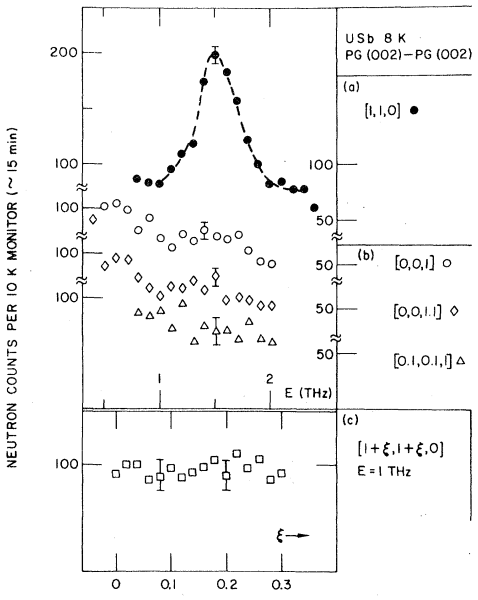

FIG. 5. (a) Constant-$\vec{Q}$ scan at the [1,1,0] point. (b) Constant-$\vec{Q}$ scans at and near the [0,0,1] point. (c) Constant-energy scan at 1 THz around the [1,1,0] point. All data taken at 8 K.

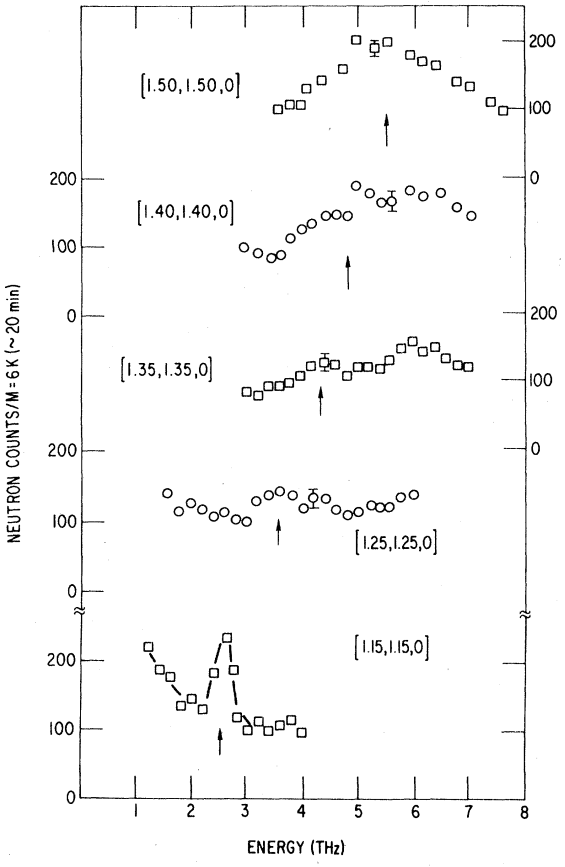

FIG. 6. Neutron groups to show propagation of collective excitation in the $[\xi,\xi,0]$ direction at 8 K. Spectra taken with Cu(111)→PG(002) and $k_f = 4.2$ Å^{-1}. The data presented are the average of several scans at each value of $\vec{Q}$.

At $[1,1,1.5]$ we see what appears to be two peaks, the longitudinal collective excitation at ~5 THz, and the broad dispersionless mode at 6–7 THz, At $[0,0,1.5]$, on the other hand, we cannot observe the longitudinal part for the reasons given above, but, by similar arguments, this shows that the mode at ~7 THz must have transverse components. The observation of scattering up to energy transfers of 9 THz with $Q = 1.5$ Å^{-1} requires small spectrometer angles ϕ and long counting times because of the reduction of incident neutron flux from the reactor above 16 THz, coupled with the decreasing efficiency of monochromators. Under these conditions, particular care has to be taken lest fast neutrons contaminate the spectra at large ΔE. The drop in intensity for $\Delta E > 8$ THz is therefore significant in Fig. 7, and shows that the broad scattering response function decreases for $\Delta E > 7.5$ THz.

The complete low-temperature magnetic-excitation spectrum is given in Fig. 8. Two types of ex-

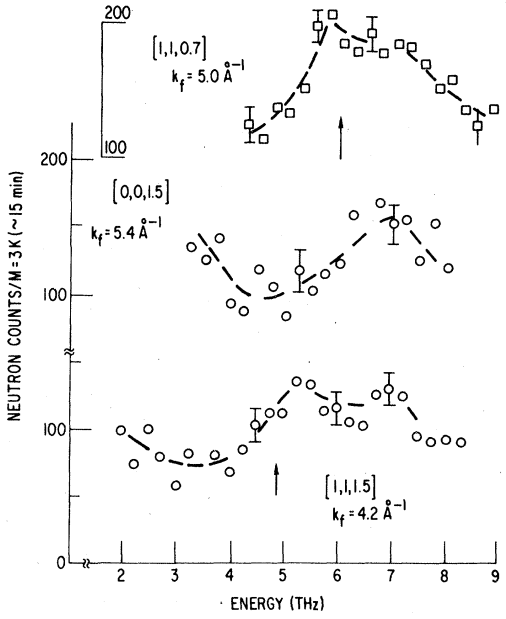

FIG. 7. Scans at high-energy transfers with Cu(111) → PG(002) showing the broad exciton level at ~6 THz. All scans taken at 8 K. The arrows indicate the positions of the collective excitation (see Fig. 8).

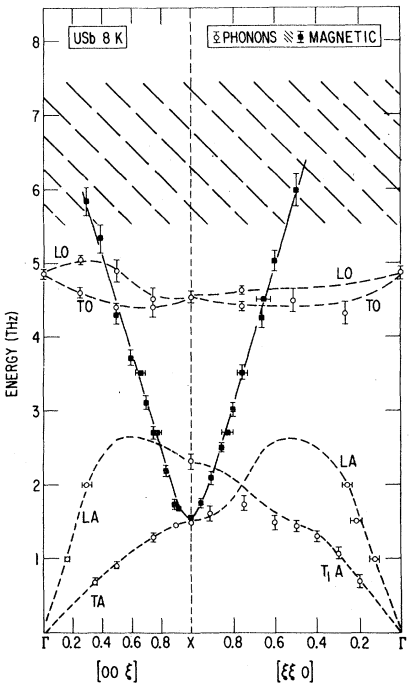

FIG. 8. The dispersion curves for USb; energy plotted against wave-vector transfer $\vec{Q}$ (in units of $2\pi/a$). The dashed lines represent the phonon dispersion and are based on the measured open points as well as on our knowledge of phonons in NaCl structures; see Ref. 25. The magnetic modes are represented by solid squares (the collective excitation) and the hatched area (excitonic level).

citations are found. Centered at the X point is a steeply rising collective excitation that is almost completely longitudinal in character. The dispersion is isotropic in the $[\xi\xi 0]$ and $[00\xi]$ directions, and, slightly away from the X point has a value of (6.7 ± 0.2) THz Å. At higher energies we observe a broad, essentially dispersionless mode (since this looks like a dispersionless crystal-field level or exciton, we shall call it that). Note that the instrumental resolution at this energy transfer is at least 1.5 THz, but we do not have enough intensity to deconvolute the experimental scans, so we cannot be sure of the intrinsic width of the exciton. The polarization of this mode has not been determined, but it must have transverse components. In Fig. 8 we have omitted the branch of the collective excitation which by symmetry is centered at the Γ point. The work of Lurie *et al.*[22] suggests that the signal at the Γ point should be very weak (out-of-phase spin waves), and, in agreement with this expectation, we were unable to detect any magnetic scattering at Γ, except the exciton mode.

C. Temperature dependence

The temperature dependence of the collective excitation at the point [1.15, 1.15, 0] is shown in Fig. 9. We have chosen this point because the excitation can be separated clearly from the incoherent elastic contribution and no phonon contribution occurs (the T_1A phonon at ~2.2 THz has a very small structure factor in this zone).

In Fig. 10 we show the results of scans with good statistics (3 repeats added together) and then fitted with a Gaussian curve to simulate the experimental resolution. At low temperature, the Gaussian width is in agreement with calculations using the experimental collimation. At higher temperatures, a slight broadening was observed, but attempts to fit the data with an experimental resolution width convoluted with a Lorentzian broadening function proved inconclusive. To obtain the intensities of the peaks, we have therefore fitted a sample Gaussian function, and the results are shown in Fig. 11. The ordered moment, as measured by the integrated intensity of the (110) Bragg peak, diminishes very slowly up to 150 K since $T_N \sim 240$ K, but the collective excitation is unobservable above 125 K.

Figure 9 shows that the frequency increases with increasing temperature. To demonstrate that the changes in intensity and frequency are not related to resolution effects, we have performed constant-energy scans at 2.7 THz, and the results are shown in Fig. 12. One can see directly from these scans that the frequency shift is greater in the [110] direction than in the [001] direction, so

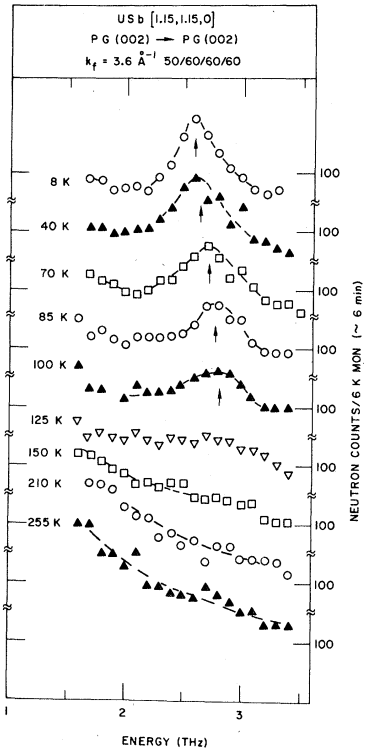

FIG. 9. The temperature dependence of the collective excitation at [1.15, 1.15, 0]; all scans taken with $k_f = 3.6$ Å^{-1}. The lines are guides to the eye. The peak width at 8 K represents the instrumental resolution.

that the dispersion is no longer isotropic at temperatures above 20 K.

The frequency dependence of the [1.15, 1.15, 0] (reduced $q = 0.215$ Å^{-1}) and the [1, 1, 0.2] (reduced $q = 0.203$ Å^{-1}) points are shown together with that

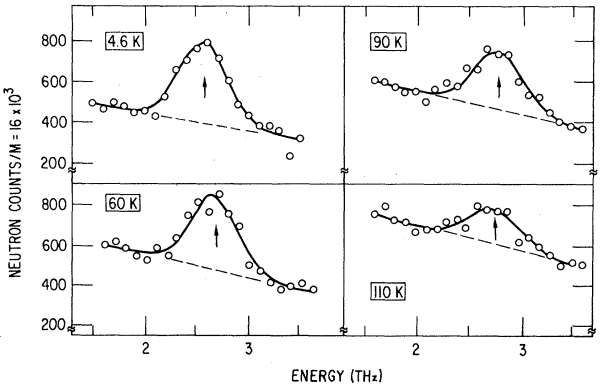

FIG. 10. Variation in frequency and intensity of the collective excitation at [1.15, 1.15, 0] as a function of temperature. The data were taken with PG(002) → PG(002) and $k_f = 3.6$ Å^{-1}. The lines are fitted Gaussian functions with the full width at half maximum kept fixed at 0.53 THz, which is the instrumental resolution.

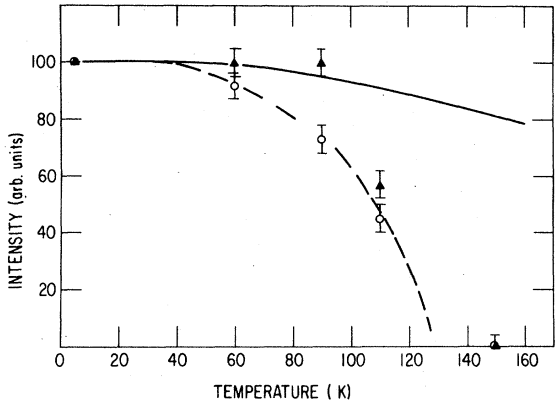

FIG. 11. Temperature dependence of the intensity of the collective excitation. Open points correspond to measurements at [1.15,1.15,0] and closed triangles to those at [1,1,0.2]. The solid line shows the decrease in the elastic intensity at the [1,1,0] position (taken from Ref. 20) and therefore corresponds to the square of the projection of the ordered moment along the [001] axis.

of the [1,1,0] in Fig. 13. The temperature dependence at the [1,1,0] point is very small.

The temperature dependence of the exciton proved difficult to measure, in part due to the increased scattering at higher temperatures from the optical phonons, and in part due to the general increase in background at higher temperatures. Given these limitations, we believe the exciton modes to be independent of temperature in both frequency and intensity.

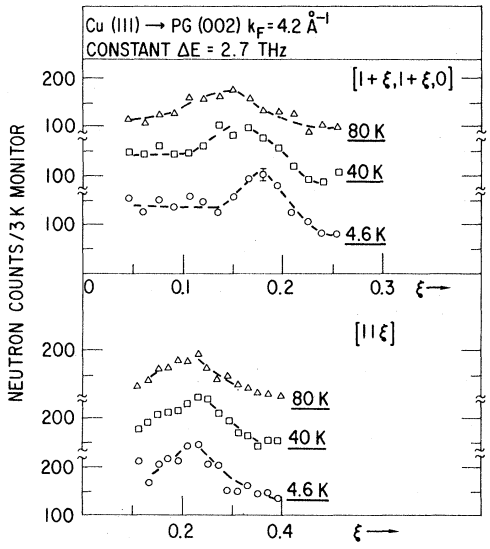

FIG. 12. Constant-energy scans (ΔE=2.7 THz) at various temperatures in the [ξ,ξ,0] and [0,0,ξ] directions. Data taken with Cu(111)→PG(002) and k_f =4.2 Å^{-1}.

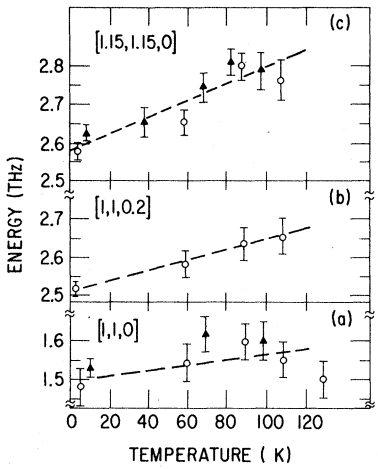

FIG. 13. Temperature dependence of the frequency of the collective excitation at different positions. Different symbols correspond to observations with different spectrometer configurations.

D. Search for magnon-phonon interaction

In Fig. 8 the excitation at the X point is shown at the same energy as the zone boundary TA (00ξ) $-LA$ ($\xi\xi$0) phonon. In fact the phonon was measured at [1,1,4] and the magnetic excitation at [1,1,0]. Acoustic phonons cannot be observed around [1,1,0] at low temperature because the

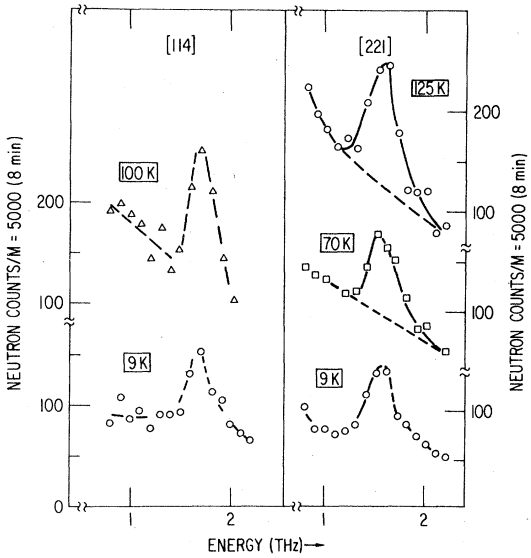

FIG. 14. Results of attempts to search for interaction between the collective excitation and the phonon at the X point. The groups at [114] are purely phonons, whereas those at [221] are mixed phonon and magnetic. See text for discussion. Data taken with PG(002)→PG (002), k_f =2.662 Å^{-1}, and a filter to eliminate higher-order contamination.

momentum transfer is too small. The question arises as to whether a magnon-phonon interaction can be observed directly, and our attempts to do this are illustrated in Fig. 14. At [114] we cannot observe the longitudinal excitation because the scattering vector is close to [001], and the magnetic form factor is small. If we define α as the angle between the spin direction [001] and $\vec{Q}$, then $\sin^2\alpha_{[114]} = 0.111$, $f^2(Q) = 0.29$, and the magnetic intensity is proportional to $f^2(Q)\sin^2\alpha = 0.035$. The signal at [114] is therefore predominantly scattering from the acoustic phonon. On increasing the temperature the intensity doubles, exactly as predicted by the Bose population factor, and the frequency remains the same. On the other hand, at the [221] point $f^2(Q)\sin^2\alpha = 0.47$, so we should expect to be able to see the magnetic excitation at low temperatures. At 125 K we can assume all the peak comes from the phonon because the intensity of the collective magnetic mode is very small (see Figs. 9 and 11), and, normalized to this value, the population factor gives that ~90% and ~70% of the peaks at 70 K and 9 K, respectively, come from phonon scattering. The remaining ~30% of the peak at 9 K is therefore magnetic scattering and this intensity is also consistent with that predicted from the [110] neutron group shown in Fig. 5, which was measured under identical conditions. Thus, although Fig. 14 shows a scan with both nuclear and magnetic excitations contributing at the same frequency, we are unable to see any interaction (in the form of line broadening or frequency shifts) between them.

E. Diffuse magnetic-response function

We have so far discussed two parts of the magnetic-response function, the collective longitudinal excitation and the exciton. Above ~80 K, a third also exists and appears to consist of a broad (in energy) featureless spectrum centered at $\Delta E = 0$. The triple-axis spectrometer is not an ideal instrument to measure such a spectrum because it essentially looks at a small region of $(\vec{Q}, \omega)$ space within which the total diffuse signal is quite weak. Nevertheless in Figs. 9, 10, and 14 the sloping background becomes most pronounced at elevated temperatures. In view of the results of Wedgwood and de Novion, who used the time-of-flight method which is more sensitive to the general features of the diffuse response function, we should not be surprised at this. In their measurements, which were mostly done at room temperature, they attempted to show that the magnetic scattering could be described as a broad Gaussian centered at $\Delta E = 0$. The separation of this rather weak magnetic signal from the phonon density of states posed great difficulties and prevented their publishing quantitative results. Nevertheless this diffuse scattering is *not* present in the isostructural, but nonmagnetic, compounds ThP and ThSe, and we believe their results are of considerable significance. Unfortunately, we have been unable to measure the intensity and half-width of this diffuse function with any reliability and plan further experiments, probably with the time-of-flight technique. The indications are that it is narrow at low temperature and gradually broadens as the temperature is raised, much like a conventional paramagnet with a Korringa relaxation mechanism. In this respect the response function appears different from that of the valence fluctuation system[14] $Ce_{1-x}Th_x$. We can say that this response function has both transverse and longitudinal components and that the collective excitation disappears into it as the temperature is raised (see Fig. 9).

IV. DISCUSSION

A. Application of previous models

In the preceeding sections we have indicated on a number of occasions that the results of this experiment are unexpected. Two previous neutron-inelastic experiments have been reported on uranium compounds. Cowley and Dolling[29] reported on the magnetic excitations in UO_2 in 1968. Uranium dioxide is an insulator with two localized $5f$ electrons and the spin-wave spectrum could be described within a conventional triplet ($S=1$) model, approximating the Γ_5 ground-state triplet of the $^3H_4$ configuration. In contrast to this reasonably well understood behavior, are the results reported[30] on UN. In this system *no collective* magnetic excitations of any type have been found; the magnetic response function consists entirely of diffuse scattering which is primarily longitudinal in nature and centered near the zone boundary acoustic phonon at [110]. The similarities between the results for USb and UN are most striking, especially when compared with the spin-wave spectra of more conventional materials. Of course, the fundamental difference between UO_2 on the one hand and USb and UN on the other, is that the latter two are metallic. It seems logical, therefore, to associate these differences with the presence of the conduction electrons and their interaction with the $5f$ band. This idea is not new,[8,9] and has received further confirmation from careful reflectivity measurements,[31] but still poses serious theoretical difficulties.

Before further discussion along these lines, let us turn to the predictions of crystal-field theory to see if they can shed any light on our experimen-

tal results. In a study of the elastic scattering from USb, Lander *et al.*[20] proposed an unusual crystal-field ground state in which the $|M=\frac{7}{2}\rangle$ was at a lower energy than the $|M=\frac{9}{2}\rangle$ state within the $5f^3$ manifold. To obtain the ordered moment an exchange field of $H_{exch}=2400$ kOe was introduced and together with the crystal-field potentials $V_4=-300$ K and $V_6=-15$ K this model gives a reasonable fit to the ordered moment, the anisotropy in the form factor, and the temperature dependence of the dipole and quadrupole moments. We can therefore calculate the matrix elements from this model which would be appropriate for the operators J_+, J_-, and J_z. These are given in Table I. Although this does not include $\vec{q}$-dependent exchange it should give us some idea of what one would see in neutron-inelastic scattering, and corresponds to the approach of Ref. 28 (see Table IV of this reference).

First note how small the J_z matrix elements are in comparison to the two large J_+ and J_- matrix elements. It is the J_z elements, of course, that give rise to longitudinal excitations. They are not small simply because of the model we have chosen, but rather *because the strong exchange field necessary to obtain the almost-free-ion ordered moment polarizes the wave functions so that they resemble single* $|M_J\rangle$ *states*. The free-ion $5f^2$ moment is $3.2\mu_B$ and the $5f^3$ value is $3.27\mu_B$, so that in USb with a $2.8\mu_B$, we have ~85% of the free-ion value, independent of whether we select a $5f^2$ or $5f^3$ configuration. This situation is demonstrated also by the studies of TbSb[28] and NdSb,[21] in which the longitudinal excitations have relatively small matrix elements. In the completely free-ion situation, as in the rare-earth metals for example, the single $|M_J\rangle$ states give rise to zero J_z matrix elements.

In summary, we can say that although the crystal-field model, in principle, gives rise to J_z matrix elements, it also predicts transverse spin waves, which are both stronger in intensity and at a lower energy than the collective longitudinal excitation. Such a prediction is in disagreement with our experimental results.

B. Relationship with critical scattering

The absence of transverse correlations has already proved to be one of the most unusual aspects of the diffuse critical scattering[32] measured near T_N. However, the absence of any measurable spin-wave response is a much more stringent restriction on $S(\vec{Q},\omega)$ than that previously observed, although the two are certainly consistent. The question arises: Where is the transverse response in this system? Two answers are possible. First, it may be represented by the exciton at ~6 THz or be at much higher energy transfer than our measurements can probe, or, second, it may be the broad low-energy magnetic scattering discussed in Sec. III E. We are unable to choose experimentally between these alternatives.

The longitudinal response function just above T_N was found to be highly anisotropic,[32] with correlations within the (001) plane much stronger than those between the (001) planes. In the ordered phase the dispersion in the [110] and [001] directions is isotropic at low temperatures, so that no simple analogy exists. Of course, the critical scattering measurements were done at [110] and were supposedly elastic only. From our discussion of the low-energy scattering in Sec. III E, we can see that this assumption is incorrect, and that the energy width is large with essentially quasi-elastic "critical" scattering superposed on it. Such a revised concept would not alter the anisotropy in the critical regime, but might contribute to incorrect values of the correlation length κ, and hence an incorrect value for the critical exponent ν as a function of temperature.

C. The exciton or crystal-field level

Have we in fact observed a crystal-field level at

TABLE I. Matrix elements of J for U^{3+} in USb based on the crystal-field model in Ref. 20.

n	E (THz)	$\langle n\|J_+\|0\rangle$	$\langle n\|J_-\|0\rangle$	$\langle n\|J_z\|0\rangle$	$\langle n\|J_z\|n\rangle$
0	0	0	0	3.45	3.45
1	3.69	0	−3.98	0	2.23
2	5.09	2.94	0	0	4.49
3	8.52	0	0	0	0.84
4	13.40	−0.60	0	0	−0.21
5	16.91	0	0	−0.44	−0.46
6	18.23	0.27	0	0	−2.78
7	18.54	0	−0.52	0	−1.23
8	18.61	0	0	0	−1.84
9	27.16	0	0	−0.01	−4.49

~6 THz (300 K)? Probably yes. Let us return to the temperature dependence of the quadrupole moment as measured in the neutron-elastic-scattering experiment.[20] In this experiment we measure the change in symmetry of the wave function as the higher levels are populated according to the Boltzmann factor. The experimental data of Ref. 20 can be understood by assuming that the wave function consists of a mixture of the ground state $|M=\frac{7}{2}\rangle$ and an excited state of predominantly $|M=\frac{9}{2}\rangle$ symmetry. The amount of mixing is governed by the factor $\exp(-\Delta/kT)$, where Δ is the energy between the two states. Since these two states have quadrupole moments of opposite signs, the magnitude of the measured (averaged) quadrupole moment will decrease as the temperature is raised. The argument concerning Δ is one primarily of symmetry and can be reproduced with any two-level scheme, provided the quadrupole moments are different. In Ref. 20 $\Delta \sim 300$ K (6 THz), which is exactly what we find for the exciton in the inelastic scattering measurements. The agreement between the two measurements is therefore excellent. Both experiments suggest that a state of different symmetry from the ground state exists with an energy separation of ~6 THz, but, of course, neither experiment identifies the complete crystal-field multiplet. Although the main results of the present neutron-inelastic experiment apparently cannot be understood within the framework of conventional crystal-field theory, this does not mean that such crystal-field states do not exist. Indeed, the strong spin-orbit coupling will definitely lead to such states. Other interactions, however, may be more important in determining the dynamic behavior.

V. SUMMARY

The results of this experiment may be summarized as follows:

(1) We have been unable to observe conventional (transverse) spin waves at energies below 8 THz. This is analogous to the situation reported[30] for UN.

(2) A longitudinal collective excitation with a minimum energy at the magnetic zone center has been observed (see Fig. 8).

(3) This excitation appears completely degenerate with the phonon at the X point, but no conventional magnon-phonon interaction appears to exist (see Fig. 14).

(4) As the temperature is increased, the intensity of this collective mode rapidly decreases (see Figs. 9–11) so that by $T_N/2$ the mode is unobservable. The frequency of the collective mode tends to increase with increasing temperature (see Fig. 13).

(5) A dispersionless (and almost temperature-independent) mode is seen at ~6 THz. We believe this to be a crystal-field transition between states with primarily $|M=\frac{7}{2}\rangle$ and $|M=\frac{9}{2}\rangle$ components, as suggested by the analysis presented in Ref. 20.

(6) We have qualitative evidence that a broad response function also exists at low energy. This becomes both stronger and more diffuse in energy as the temperature is raised. Such a response function has already been observed in time-of-flight measurements on these compounds,[5] as well as in the experiments[30] on single crystals of UN.

ACKNOWLEDGMENTS

We are particularly grateful to Oscar Vogt for growing these crystals and his continued interest in the project. It is a pleasure to thank W. J. L. Buyers, B. R. Cooper, T. M. Holden, and S. K. Sinha for many useful discussions. The technical assistance of A. Brochier and B. Wanzel is gratefully acknowledged and we thank the Institut Laue Langevin for the use of its facilities. The work of G. H. Lander was supported in part by the U. S. Department of Energy.

---

* Permanent address.

[1] B. G. Wybourne, *Spectroscopic Properties of Rare Earths*, (Interscience, New York, 1965), p. 198 ff.

[2] J. Grunzweig-Genossar, M. Kuznietz, and F. Friedman, Phys. Rev. 173, 562 (1968).

[3] S.-K. Chan and D. J. Lam, in *The Actinides Electronic Structure and Related Properties*, edited by A. J. Freeman and J. B. Darby (Academic, New York, 1974), Vol. I., p. 1 ff.

[4] See, for example, many references in *Crystal-Field Effects in Metals and Alloys*, edited by A. Furrer (Plenum, New York, 1977).

[5] F. A. Wedgwood, J. Phys. C 7, 3203 (1974); F. A. Wedgwood and C. H. de Novion (unpublished).

[6] See G. H. Lander in Ref. 4, p. 213 for a summary table of measurements performed. Recently crystal-field levels have been seen in UPd_3 [N. Shamir, M. Melamud, H. Shaked, and M. Weger, Physica 94B, 225 (1978)]. See also A. F. Murray and W. J. L. Buyers, in Proceedings of the International Conference on Crystalline Electric Fields, Philadelphia, 1979 (Plenum, New York, to be published).

[7] A. Furrer and A. Murasik, Helv. Phys. Acta 50, 447 (1977).

[8] H. L. Davis in Ref. 3, Vol. II, p. 1.

[9] D. E. Eastman and M. Kuznietz, Phys. Rev. Lett. 26,

846 (1971).
[10]G. H. Lander and D. J. Lam, Phys. Rev. B 14, 4064 (1976).
[11]D. J. Lam and A. T. Aldred in Ref. 3, Vol. I, p. 109.
[12]J. M. Fournier, A. Blaise, W. Muller, and J. C. Spirlet, Physica 86-88B, 30 (1977); B. Kanellakopoulas, A. Blaise, J. M. Fournier, and W. Muller, Solid State Commun. 17, 713 (1975).
[13]E. Holland-Moritz, M. Loewenhaupt, W. Schmatz, and D. K. Wohlleben, Phys. Rev. Lett. 38, 982 (1977).
[14]S. M. Shapiro, J. D. Axe, R. J. Birgeneau, J. M. Lawrence, and R. D. Parks, Phys. Rev. B 16, 2225 (1977).
[15]B. C. Sales and D. K. Wohlleben, Phys. Rev. Lett. 35, 1240 (1975).
[16]M. E. Foglio, J. Phys. C 11, 4171 (1978).
[17]J. M. Robinson, Phys. Rep. 51, 1 (1979).
[18]J. M. Robinson and P. Erdos, Phys. Rev. B 8, 4333 (1973); Phys. Rev. B 9, 2187 (1974).
[19]G. H. Lander, W. G. Stirling, and O. Vogt, Phys. Rev. Lett. 42, 260 (1979).
[20]G. H. Lander, M. H. Mueller, D. M. Sparlin, and O. Vogt, Phys. Rev. B 14, 5035 (1976).
[21]A. Furrer, W. J. L. Buyers, R. M. Nicklow, and O. Vogt, Phys. Rev. B 14, 179 (1976).
[22]N. A. Lurie, G. Shirane, P. Heller, and A. Linz, AIP Conf. Proc. 10, 93 (1973).
[23]H. G. Smith and W. Glaser, in *Proceedings of the International Conference on Phonons, Rennes,* edited by M. A. Nusimovici (Flammarion, Paris, 1971), p. 145.
[24]G. Dolling, T. M. Holden, E. C. Svensson, W. J. L. Buyers, and G. H. Lander, in *Proceedings of the International Conference on Lattice Dynamics, Paris, 1977,* edited by M. Balkanski (Flammarion, Paris, 1978), p. 81.
[25]G. Raunio and S. Rolandson, J. Phys. C 3, 1013 (1970).
[26]G. Peckham, Proc. Phys. Soc. (London) 90, 657 (1967).
[27]M. P. Schulhof, R. Nathans, P. Heller, and A. Linz, Phys. Rev. B 4, 2254 (1971), and references therein.
[28]T. M. Holden, E. C. Svensson, W. J. L. Buyers, and O. Vogt, Phys. Rev. B 10, 3864 (1974).
[29]R. A. Cowley and G. Dolling, Phys. Rev. 167, 464 (1968).
[30]W. J. L. Buyers, T. M. Holden, E. C. Svensson, and G. H. Lander, *Proceedings of the International Conference on Neutron Inelastic Scattering* (International Atomic Energy Agency, Vienna, 1978), p. 239.
[31]J. Schoenes and O. Vogt, Solid State Commun. 28, 261 (1978).
[32]G. H. Lander, S. K. Sinha, D. M. Sparlin, and O. Vogt, Phys. Rev. Lett. 40, 523 (1978).